Dielectric properties of lithium triborate single crystals

Ji Won Kim, Choon Sup Yoon, and H. G. Gallagher

Citation: Appl. Phys. Lett. **71**, 3212 (1997); doi: 10.1063/1.120293
View online: http://dx.doi.org/10.1063/1.120293
View Table of Contents: http://apl.aip.org/resource/1/APPLAB/v71/i22
Published by the American Institute of Physics.

Dielectric properties of lithium triborate single crystals

Ji Won Kim and Choon Sup Yoon[a)]
Department of Physics, KAIST, Daeduck Science Town, Taejon, 305-701 Korea

H. G. Gallagher
Department of Physics and Applied Physics, University of Strathclyde, Glasgow GI IXN, Scotland, United Kingdom

(Received 12 August 1997; accepted for publication 1 October 1997)

From the impedance analysis, we report the dielectric constants of lithium triborate single crystals for the three principal axes in the frequency range of 100 Hz–1 MHz and in the temperature range of 303–773 K. The observed highly anisotropic behavior of dielectric dispersions is mainly related to the anisotropy of the activation energy for Li^+ ion hopping, which is constituted by the B_3O_7 channel framework lain along the *c* axis. © *1997 American Institute of Physics.* [S0003-6951(97)01948-7]

Lithium triborate [LiB_3O_5 (LBO)] is a nonlinear optical crystal and has received considerable attention because of its interesting optical properties such as a relatively large second-order nonlinear optical coefficient ($d_{\text{eff}}=1.4$ pm/V),[1,2] high optical damage threshold (25 GW/cm,[2] 1.064 μm, 0.1 ns),[3] wide transparency range (0.16–3.5 μm),[1] very small walk-off angle, and large acceptance angle for phase matching.[1,2]

The optical properties[1–3] and the applications to harmonic and parametric generations[4] of LBO have been investigated intensely. Other physical properties such as infrared reflectance,[5] Raman spectra,[5] interband conductivity,[6] and elastic and piezoelectric properties[7] were also studied. Although dielectric constants are considered to be one of the fundamental quantities that represent the electrical properties of a material, to the best of our knowledge, no literature has yet reported the dielectric properties of LBO crystals. In this letter, we report the complete measurements of the dielectric constants in the frequency range of 100 Hz–1 MHz and in the temperature range of 303–773 K.

The imaginary part of the dielectric constant ϵ'' is related to the ionic conductivity σ as

$$\epsilon''=[\sigma(\omega)-\sigma(0)]/\omega\epsilon_0, \tag{1}$$

where $\sigma(0)$ is the dc conductivity, ω is the frequency of the applied electric field, and ϵ_0 is the dielectric permittivity of free space. Furthermore, the ionic conductivity σ is related to the diffusion coefficient through the Nernst–Einstein relation as $\sigma=N(Ze)^2D/k_BT$, where N is the total number of the charge carriers, Ze is the charge of the carrier ($Z=1$ for LBO), and D the diffusion coefficient of mobile ions. So, the conductivity has a simple form as

$$\sigma\cdot T=A\ \exp(-\Delta H/k_BT), \tag{2}$$

where ΔH is the activation energy for ionic hopping and A is the constant, which is a function of the total number of the charge carriers, ionic jump frequency, and the hopping distance.

LBO crystals of $30\times30\times25$ mm^3 size and of high perfection were grown by the top seeded solution growth method at the authors' laboratory. The perfection of the grown LBO crystals was characterized by using synchrotron x-ray topography, and the dislocation density was analyzed to be less than 10/cm^2.

LBO crystals belong to the orthorhombic space group $Pna2_1$ and point group mm2 with cell parameters $a=8.4473$ Å, $b=7.3788$ Å, $c=5.1395$ Å, and $Z=1$.[1] Thin plate samples were cut and polished perpendicular to the three principal axes. The thickness of the samples was less than 0.2 mm and the area was about 6×6 mm^2 for all samples. Difficulties with obtaining reproducible dielectric data were encountered for heating and cooling runs, and this was found to be associated with the inhomogeneous distribution of vacancies in LBO crystals, which provide hopping sites for Li^+ ions.[6] The introduction of the annealing proce-

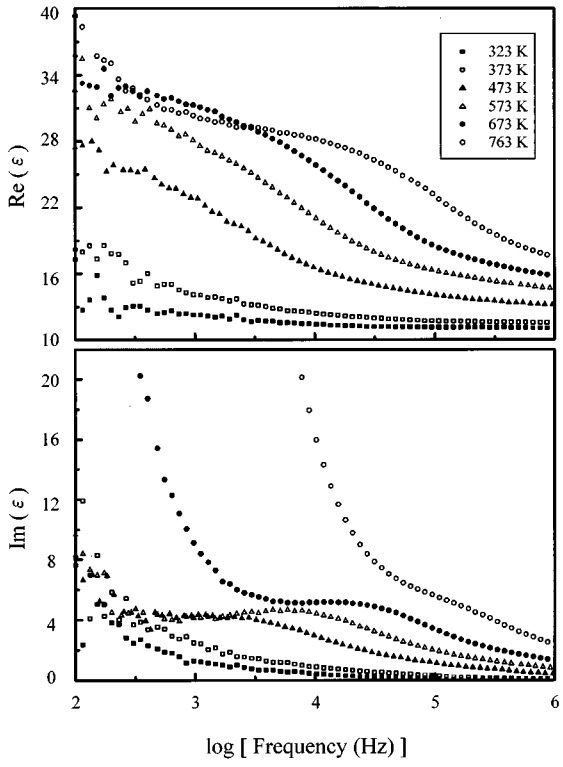

FIG. 1. The dispersion of the dielectric constant for the *a* axis.

[a)]Electronic mail: csyoon@convex.kaist.ac.kr

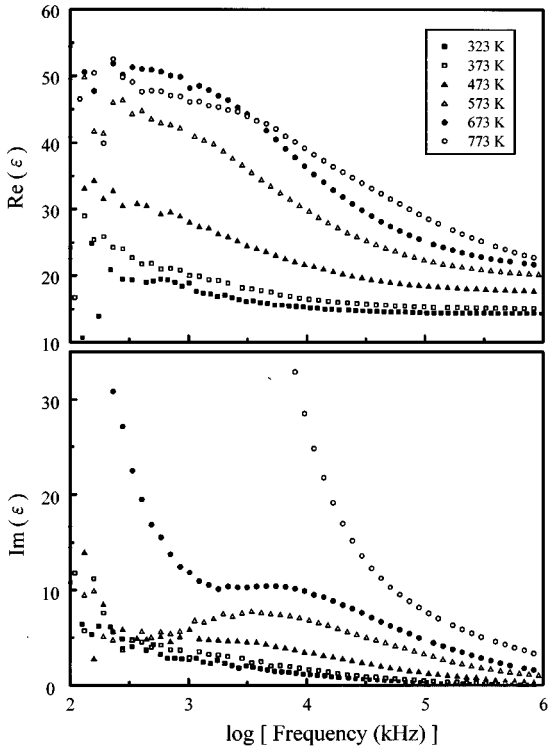

FIG. 2. The dispersion of the dielectric constant for the *b* axis.

dure was, therefore, essential for reproducible data, and all the samples used were annealed at 923 K for 7 h before evaporating the gold electrodes of 1 μm thickness and 4.5 $\times$4.5 mm^2 area.

An impedance analyzer (Hewlett Packard, HP4192A) was used to measure the real and imaginary parts of the dielectric constants, and the samples were placed in the electrically shielded oven in which the temperature was controlled to within $\pm$0.1 K by the Eurotherm 903P temperature controller. Measurements were done in the frequency range of 100 Hz – 1 MHz with 200 samplings, and at every 10 K in the temperature range of 303–773 K. The rate of temperature increase for the samples was 0.3 K/min.

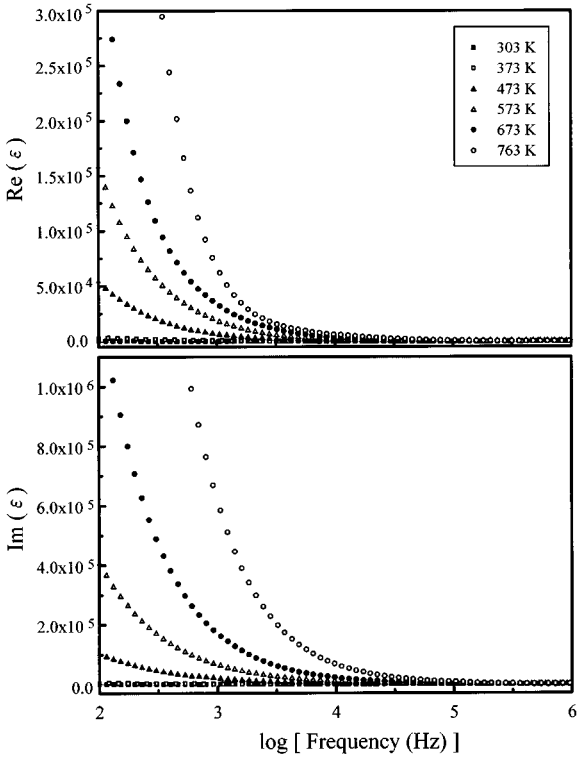

FIG. 3. The dispersion of the dielectric constant for the *c* axis.

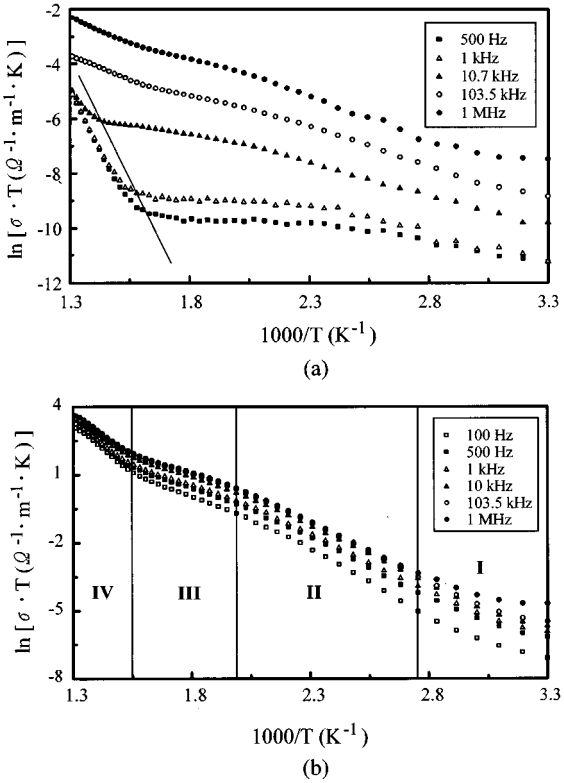

FIG. 4. Temperature dependence of the ionic conductivity (a) along the *a* axis and (b) along the *c* axis.

The dispersions of the dielectric constants for the *a*, *b*, and *c* axes are shown in Figs. 1–3. As shown in Figs. 1 and 2, the dielectric behavior for the *b* axis is very similar to that for the *a* axis, and the broad relaxation peaks appear below 600 K for both axes. However, there appears no relaxation peak for the *c* axis (Fig. 3), and the real and imaginary parts of the dielectric constants show a typical low-frequency dispersion behavior.[8] The dielectric constants at 1 MHz are 11.06, 14.29, and 10.71 at 323 K, and 17.53, 22.36, and 37.35 at 763 K for the *a*, *b*, and *c* axes, respectively.

The temperature dependence of ac conductivity was derived from the relation (1) and is depicted in Fig. 4 for the *a* and *c* axes. The conductivity plot for the *b* axis is not included since it is very similar to that for the *a* axis. It is clearly seen that the overall conductivities for the *c* axis are several orders of magnitude larger than those for the *a* axis. For example, at $f=500$ Hz and at 373 K, the conductivity for the *c* axis is 5.8×10^{-5} Ω^{-1} m^{-1}, while the conductivity for the *a* axis is 9.5×10^{-8} Ω^{-1} m^{-1}.

Figure 4(a) shows that the conductivity versus temperature curves for $f=500$ Hz, 1 kHz, and 10.7 kHz consist of two parts of a different slope. The initial linear portion with a steep gradient at high temperatures is due mainly to the

TABLE I. Activation energy for the different temperature ranges.

Regime	Temperature range (K)	Activation energy (eV) 100 Hz	1 MHz
I	300–363	0.23	…[a]
II	363–503	0.55	0.42
III	503–643	0.31	0.25
IV	643–773	0.75	0.63

[a]Estimation is not available owing to insufficient data points.

Arrhenius-type ion conduction process. On the other hand, the low-level portion with a very moderate gradient is ascribed to the localized hoppings of Li^+ ions. This localized hopping is responsible for the broad dielectric relaxation peaks in the dispersion curves of the imaginary part of the dielectric constants below 600 K in Figs. 1 and 2. The temperatures at which the conducting mechanisms change from the Arrhenius type to the localized hopping type go higher as the frequency becomes larger, as indicated by the solid line in Fig. 4(a), since the larger the frequency, the greater the thermal energy required for successive hoppings. The conductivity plot as a function of temperature for the *c* axis in Fig. 4(b) clearly demonstrates that the conduction process is Arrhenius type. Four regimes of different slopes are identified over the full temperature range with different activation energies. Also, the different slope for the different frequency curve implies the dispersion of the activation energy. In Table I, the activation energy derived from Eq. (2) for the different regimes is summarized.

It has been reported that Li^+ ion mobility is responsible for the conductivity in LBO crystals,[6] and in other borate crystals and glasses.[9,10] The observed highly anisotropic behaviors of dielectric constants and conductivities for the *a* (or *b*) and *c* axes are associated with the structural characteristics of a LBO crystal. An analysis[6] of the crystal structure of LBO reveals that $[BO_3]$ triangles and $[BO_4]$ tetrahedra constitute a three-dimensional channel framework along the *c* axis with the Li^+ ions inside so that the Li^+ ions can hop to the neighboring vacancy sites in the channel direction with little interactions. So, ac conductivities along the *c* axis show very little dispersive behavior even at low temperatures. However, for the directions perpendicular to the *c* axis, the Li^+ ions find it difficult to hop to the neighboring sites across the framework, which results in small conductivity values. Although hopping can succeed at high temperatures, strong ion–lattice interactions cannot be avoided. As a consequence,[11] there appears a strong dispersion in the ac conductivity along the *a* and *b* axes. Before the successive hopping of the Li^+ ions takes place, a localized hopping can happen. This induces the shifting of the Coulomb-cage potential by the lattice relaxation,[11] and the non-Debye-type broad peaks in Figs. 1 and 2 appear due to this effect.

In conclusion, complete dielectric constant measurements have been made on LBO crystals, and the dielectric dispersion and ac conductivity were discussed in association with the Li^+ ion hoppings and the ion–lattice interactions.

This work was supported in part through the HAN project and in part by the Korea Science and Engineering Foundation through the Research Center for Dielectric and Advanced Matter Physics (RCDAMP).

[1] C. Chen, Y. Wu, A. Jiang, B. Wu, G. You, R. Li, and S. Lin, J. Opt. Soc. Am. B **6**, 616 (1989).
[2] S. Zhao, C. Huang, and Z. Hongwu, J. Cryst. Growth **99**, 805 (1990).
[3] Y. Furukawa, M. Sato, and A. Markgraf, Proc. SPIE **2379**, 245 (1995).
[4] G. Robertson, A. Henderson, and H. Dunn, Appl. Phys. Lett. **60**, 271 (1992).
[5] X. Xiong, G. Lan, and H. Wang, J. Raman Spectrosc. **24**, 85 (1993).
[6] S. F. Radaev, N. I. Sorokin, and V. I. Simonov, Sov. Phys. Solid State **33**, 2024 (1991).
[7] Y. Wang, Y. J. Jiang, Y. L. Liu, F. Y. Cai, and L. Z. Zeng, Appl. Phys. Lett. **67**, 2462 (1995).
[8] A. K. Jonscher, IEEE Electron. Insul. Mag. **6**, 16; **6**, 24; **6**, 19 (1990).
[9] D. P. Button, L. S. Mason, H. L. Tuller, and D. R. Uhlmann, Solid State Ionics **9&10**, 585 (1983).
[10] S. Furusawa, S. Tange, Y. Ishibashi, and K. Miwa, J. Phys. Soc. Jpn. **59**, 2532 (1990).
[11] K. Funke, Solid State Chem. **22**, 111 (1993).